

**On-off intermittency and intermingledlike basins in a granular medium**

Malte Schmick\*

*Max-Planck-Institut für molekulare Physiologie, Postfach 500247, 44202 Dortmund, Germany*

Eric Goles†

*Centre for Mathematical Modelling, UMR 2071, CNRS–Universidad de Chile, Casilla 170-3, Santiago, Chile*

Mario Markus‡

*Max-Planck-Institut für molekulare Physiologie, Postfach 500247, 44202 Dortmund, Germany*

(Received 6 June 2002; published 20 December 2002)

Molecular dynamic simulations of a medium consisting of disks in a periodically tilted box yield two dynamic modes differing considerably in the total potential and kinetic energies of the disks. Depending on parameters, these modes display the following features: (i) hysteresis (coexistence of the two modes in phase space); (ii) intermingledlike basins of attraction (uncertainty exponent indistinguishable from zero); (iii) two-state on-off intermittency; and (iv) bimodal velocity distributions. Bifurcations are defined by a cross-shaped phase diagram.

DOI: 10.1103/PhysRevE.66.066214

PACS number(s): 05.45.–a, 45.70.–n, 47.54.+r, 47.52.+j

**I. INTRODUCTION**

Granular media are of great technological and scientific interest, most of their peculiar collective behavior not occurring in liquids or solids. (For reviews, see Refs. [1–4].)

A number of researchers have found hysteresis, and thus coexisting attractors in granular media [5–13]. In a recent work, where we considered four or less disks in a two-dimensional periodically tilting box, we reported on hysteresis involving the coexistence of an ordered and a disordered state [14]. We showed in that work that there exist parameters for which the system hops aperiodically between these two states (on-off intermittency); for other parameters, we found that any neighborhood of an initial condition leading to one state contains initial conditions leading to the other state. We demonstrated that this latter phenomenon occurred in our case due to the fact that initial inaccuracies (existing both in simulations and in experiments) are amplified during highly disordered transients, so as to become as large as the whole system within a time smaller than the transient (see also Ref. [15]); the basins of attraction thus behave as if they were intermingled [16–19] because of the unavoidable limitations in accuracy.

Our previous work with the tilting box [14] had two strong restrictions: (i) We considered only  $\nu=1, 2, 3$ , or 4 disks, so that we excluded the collective behavior emerging in granular media; and (ii) we hold the length  $b$  of the edge of the square box to  $b=2R(\nu+1)$ , where  $R$  is the radius of the disks. The reason for this latter restriction was that a smaller box considerably restricts the movement of the disks, while a larger box diminishes the number of collisions and thus reduces the disordering that is necessary for intermingling.

In the present work we investigate a system such as that presented in Ref. [14], but with a much larger number  $\nu$  of particles, so that we can consider it as a granular medium. Furthermore, we will loosen our restriction of a fixed value of  $b$  and will thus look at the influence of the size of the box at a fixed number of particles.

**II. METHODS**

We consider a two-dimensional square box oscillating around a pivot  $P$ , as illustrated in Fig. 1(a). This oscillation is described by  $\phi=A \cos(2\pi t/\tau)$ , where  $\phi$  is the angle between the vertical line passing through  $P$  (shown as a continuous line) and the straight line connecting  $P$  with the tip  $T$  (shown dashed).  $\nu=105$  disks are placed inside this box, and simulations are performed using molecular dynamics [20]. Each disk is described by its position  $\vec{r}_i$ , its velocity  $\vec{v}_i$  and the magnitude of its angular velocity  $|\vec{\omega}_i|$ . For the disk-disk and the disk-edge interactions we use the same parameters and force laws as in Ref. [14], where we had motivated the models's assumptions in accordance with optimizations and experiments given in Refs. [21,22]. We set  $R=5 \times 10^{-3}$  m, the density  $\rho$  to  $2.5 \times 10^3$  kg m $^{-3}$  and  $\tau=0.25$  s. If the overlap  $\zeta=2R-|\vec{r}_i-\vec{r}_j|>0$ , then the disks repel each other with a normal force equal to  $\vec{F}_n^{(i)}=[Y\zeta^{3/2}-\gamma_n\sqrt{\zeta}(\vec{v}_i-\vec{v}_j)\hat{n}]\hat{n}$  (Hertz theory with viscoelastic dissipation [23]).  $\hat{n}=(\vec{r}_i-\vec{r}_j)/|\vec{r}_i-\vec{r}_j|$ ,  $Y=10^5$  kg m $^{-1/2}$  s $^{-2}$ ,  $\gamma_n=30$  kg m $^{-1/2}$  s $^{-1}$ . The shear force is given by  $\vec{F}_s^{(i)}=-\hat{v}_s \cdot \min(\gamma_s|\vec{v}_s|, \nu_s|\vec{F}_n^{(i)}|)$ , where  $\hat{v}_s=\vec{v}_s/|\vec{v}_s|$ .  $\vec{v}_s=\vec{v}_i-\vec{v}_j-[(\vec{v}_i-\vec{v}_j)\hat{n}]\hat{n}+R\hat{n} \times (\vec{\omega}_i+\vec{\omega}_j)$  is perpendicular to  $\hat{n}$ . The first argument of the shear force describes the viscous flow and the second one the Coulomb sliding friction.  $\gamma_s=20$  kg s $^{-1}$ ;  $\nu_s=0.45$ . The interaction with an edge was computed as an interaction with a symmetrically placed disk. The integration time step was set to  $10^{-5}$  s using a Gear predictor-corrector algorithm [20].

For the characterization of the basins of attraction, we

\*Electronic address: schmick@mpi-dortmund.mpg.de

†Electronic address: egoles@dim.uchile.cl

‡Electronic address: markus@mpi-dortmund.mpg.de

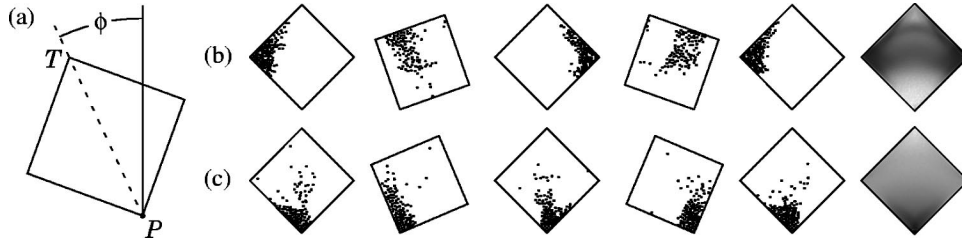


FIG. 1. (a) Scheme of the mechanical device. The tip  $T$  of a square box oscillates around the pivot  $P$ ;  $\phi = A \cos(2\pi t/\tau)$ . (b) “Ping-pong” mode. (c) “Quasiconfined” mode. (b),(c)  $A = 26.5^\circ$ ,  $b = 80R$ . From left to right:  $\phi = 0, A, 0, -A, 0$ ; the last pictures show the probability density for the position of the particles.

checked the scaling law  $f(\epsilon) \propto \epsilon^\alpha$ , where  $\alpha$  is the so-called uncertainty exponent (see, e.g., Refs. [14,15,17,19]).  $f(\epsilon)$  is the probability that two initial points in phase space lead to different attractors;  $\epsilon$  quantifies the distance between these points. An indication for intermingling of basins is that  $\alpha$  is close to zero.

The initial conditions here were set by placing the disks inside the box in a hexagonal grid within an equilateral triangle. Each side of this triangle consisted of 14 disks. For all initializations, one side of the triangle was parallel to the lower right edge of the box. The box starts its tilting motion at  $\phi = A$ . In order to quantify the initial conditions, we used the Cartesian coordinate system  $C$  with origin at  $P$  and  $x$  axis corresponding to the lower right edge of the box. For the evaluation of  $f(\epsilon)$  we considered (in  $C$ )  $N$  initial positions  $\vec{x}_k$  and  $\vec{x}_k + \vec{\epsilon}_r$  ( $k = 1, 2, \dots, N$ ) of the disk at the lowest corner of the triangle. Note that the initial conditions are contained in the phase subspace in which all disks are within the equilateral triangle and all velocities, relative to the box, are zero. We placed the  $\vec{x}_k$  equidistantly on the considered region of the plane. For each  $\vec{x}_k$  and a given  $\epsilon$ ,  $\vec{\epsilon}_r$  was chosen randomly, such that  $|\vec{\epsilon}_r|$  was uniformly distributed within  $]0, \epsilon]$ .

### III. RESULTS

In the parameter domain investigated here ( $A \leq 45^\circ$ ,  $50R \leq b \leq 130R$ ), we found two dynamic modes. In one of them, which we call “pingpong” (PP) mode, the particles are launched back and forth between the right and the left corner of the box, as illustrated in Fig. 1(b). In the other one, which we call “quasiconfined” (QC) mode, the particles stay in the neighborhood of the pivot  $P$ , as illustrated in Fig. 1(c).

For both modes we obtain clustering due to inelastic collapse, as in other granular media (see, e.g., Ref. [24]): a

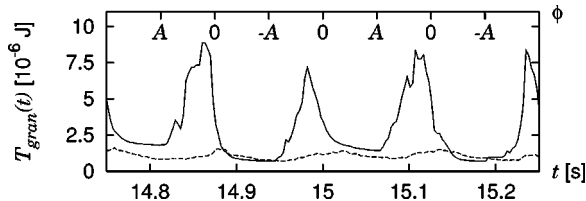


FIG. 2. Granular temperature  $T_{gran}$  vs time  $t$  for the “ping-pong” mode (continuous curve) and for the “quasiconfined” mode (dashed curve). Upper horizontal scale: angle  $\phi$ . [Parameters as in Figs. 1(b) and 1(c).]

concentration of particles increases the energy loss due to collisions, which in turn favors their concentration. In the QC mode, a cluster (sliding along the edges around  $P$ ) is present at all times, while a fraction of the particles accompanies it in a gaslike state [see Fig. 1(c)]. Contrarily, for the PP mode a gaslike state occurs for all particles when  $|\phi|$  changes from  $A$  to zero [right after the second and fourth pictures in Fig. 1(b)] and alternates with clustering. Clustering is strongest for  $\phi = 0$  [vertical  $\overline{PT}$ ; first, third, and fifth pictures in Fig. 1(b)] because then cooling is most strongly supported by inelastic collisions with the edges ( $|d\phi/dt|$  is maximum).

Figure 2 illustrates the time dependence of the granular temperature  $T_{gran}$ , which is defined as the kinetic energy (averaged over all disks), considering the disk velocities relative to the center of mass.  $T_{gran}$  for the two attractors are low and similar [ $\approx 1 - 2 \times 10^{-6}$  J] when most of the disks are confined in a corner of the box. In the QC mode (dashed curve in Fig. 2) there is slight increase of  $T_{gran}$  for  $\phi = 0$ , since then gravity minimizes the lever arm of the box edges; this minimizes the energy losses by collisions with the edges and causes a (slight) increase of the number of disks that go into the hotter, gaslike state. In the PP mode (continuous curve in Fig. 2) there is a much larger (nearly threefold) increase of  $T_{gran}$ ; this occurs when all disks are detached from the edges of the box and go into a gaslike state (see preceding paragraph).

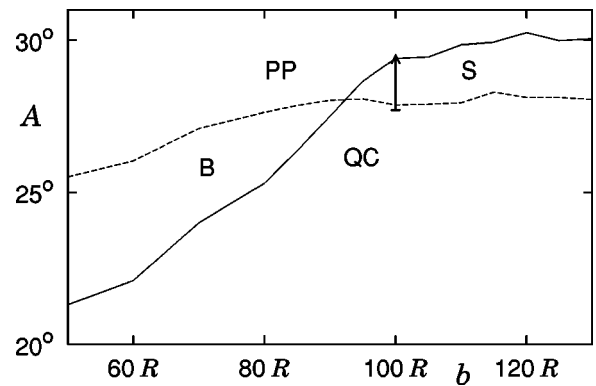


FIG. 3. Regions in parameter space. (A, oscillation amplitude;  $b$ , length of the edge of the box.) The arrow indicates the change in conditions corresponding to Fig. 5. QC: the “quasiconfined” mode is the only attractor. PP: the “ping-pong” mode is the only attractor. B: the two attractors coexist. S: there is intermittent switching between the two modes.

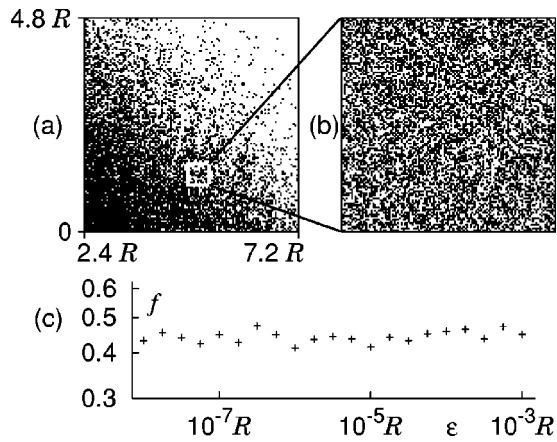


FIG. 4. (a) Basins of attraction for the “quasiconfined” mode (black) and for the “ping-pong” mode (white).  $R$ : radius of the disks;  $A = 24^\circ, b = 60R$ . (b) Enlargement showing the intermingling of the basins. (c) Probability  $f$  (evaluated with  $N = 1000$ ) that two initial conditions in (b) lead to different attractors vs the maximum distance  $\epsilon$  between these points.

The appearance of the PP and of the QC mode, depending on  $A$  and  $b$ , is shown in Fig. 3. In the region  $B$  there is birhythmicity, i.e., both modes coexist as attractors. In the region  $S$ , both modes are repellers and there are no other modes; in this region the system switches in an aperiodic way between the PP and the QC mode, i.e., the so-called two-state on-off intermittency takes place [17].

Basins of attraction in phase space, occurring in region  $B$  of Fig. 3, are illustrated in Fig. 4. Figures 4(a) and 4(b) show the fates of the system after setting the initial conditions  $\vec{x}_k$  in the displayed regions of the plane (the coordinate system is  $C$ , as defined in Sec. II). Figure 4(a) shows that placing the initial triangle close to  $P$  leads to the QC mode [black region at the lower left of Fig. 4(a)], while placing it farther up leads

to the PP mode [white region at the upper right of Fig. 4(a)]. As illustrated in Fig. 4(a) and in the enlargement in Fig. 4(b), we found a region between the black and the white domains in which we could not detect white or black open sets. In other words, in any neighborhood of an initial configuration leading to the PP mode there exists an initial configuration leading to the QC mode, and vice versa. This is a behavior also found for intermingled basins [16–18]. A quantification is given in Fig. 4(c); here, we show that the probability  $f$  is independent of  $\epsilon$ , i.e., the uncertainty exponent  $\alpha$  is indistinguishable from zero. This means that any increase in the accuracy of the initial conditions is of no help for improving predictability of the attracting mode. Closer inspection revealed that this behavior is caused here by the same reasons as in Refs. [14,15] (see Sec. I). In fact, disk-disk collisions amplify initial inaccuracies to sizes as large as the whole system within times much shorter than the transients taking place before the PP or QC modes are reached.

Choosing the situation in Fig. 1 to compare the coexisting attractors from the energetic point of view, we found that there the total energies (averaged over time) of the two modes differ by a factor of 4.0. In particular, the total potential energies differ by a factor of 2.4 and the total kinetic energies by a factor of 5.3. We set the potential to zero at the minimum obtained by starting from 1000 random distributions of the disks in the box and setting (for  $A = 26.5^\circ$  and  $b = 80R$ ) the period equal to  $\tau = 2$  s, which is long enough to prevent the gaslike behavior.

Figure 5 illustrates the changes of the system’s behavior as region  $S$  is crossed by holding  $b$  constant and increasing  $A$  along the arrow shown in Fig. 3. The upper pictures show typical time series for the center of mass, the pictures in the middle are stroboscopic plots of phase variables of the center of mass, and the lower pictures are the corresponding velocity distributions. In Fig. 5(a) (lowest  $A$ ) only the QC mode is

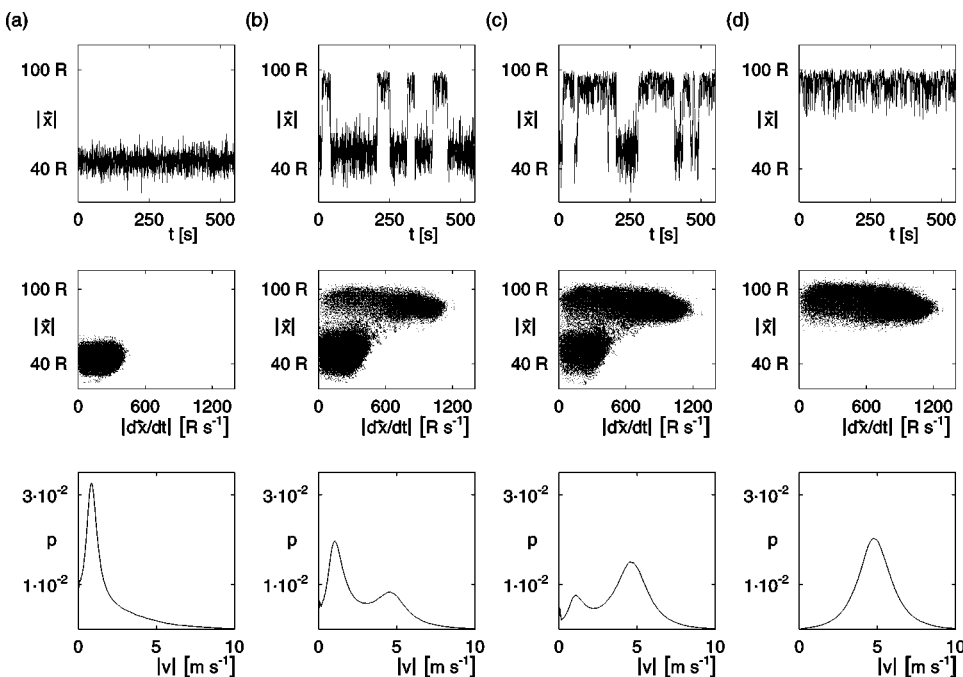


FIG. 5. Modes for increasing  $A$  at constant  $b = 100R$  and crossing region  $S$ , as shown by the arrow in Fig. 3. All scales are linear.  $\vec{x}$ : vector pointing from the pivot  $P$  to the center of mass. Upper pictures: time series of the distance  $|\vec{x}|$ . Middle: stroboscopic plots for  $|\vec{x}|$  and  $|d\vec{x}/dt|$ ; 40 points per box-tilting period are plotted. Lower pictures: probability distribution of the magnitudes of the particle velocities. (a)  $A = 27.7^\circ$  (region QC in Fig. 3). (b)  $A = 28.5^\circ$  (region  $S$  in Fig. 3). (c)  $A = 28.7^\circ$  (region  $S$ ). (d)  $A = 29.5^\circ$  (region PP in Fig. 3).

an attractor. In Figs. 5(b) and 5(c) the system hops aperiodically between the QC and the PP mode; it spends most of the time in the QC mode in the case of Fig. 5(b), and most of the time in the PP mode in the case of Fig. 5(c). (Note the corresponding changes in the bimodal velocity distributions.) In Fig. 5(d) (largest  $A$ ), only the PP mode is an attractor.

#### IV. DISCUSSION

Some of the features of our system have been reported for other granular media. These features are: hysteresis (see Refs. [5–13]), bimodal velocity distributions (as in Ref. [25]) and simultaneous existence of clustered and gaslike particles (see Refs. [6,26]). Note that simultaneous appearance of low-speed and high-speed particles does not always imply a bimodal velocity distribution, but may be observable as a deformation of the tails of a one-peaked Maxwell-distribution (see, e.g., Ref. [27]). Note also that the existence of two granular temperatures may be associated with differently sized particles, the temperature of the larger particles being higher than that of the smaller ones [28].

In addition, we found features which have—to our knowledge—not been reported so far in conjunction with granular media. These are intermingledlike basins and two-state on-off intermittency. On-off intermittency has been reported in a number of contexts involving nongranular systems; examples are: single particles in particular potentials [17,18], coupled maps [29], a mechanical system involving

springs [19], optical systems [30], one-dimensional maps [31] and dynamo models of stellar activity [32], discharge plasmas [33], and electrical circuits [34]. It is remarkable that intermittency occurs in the present system for an interval of the oscillation amplitude  $A$  that is 20 times larger than for the system investigated previously with four disks or less [14].

As a final note, we remark that the diagram in Fig. 3 can be associated with the cross-shaped phase diagrams that are used for the design of chemical oscillators [35,36]. In those cases, only two phase variables are involved, so that chaos is not possible. Instead, there exist two steady states displaying hysteresis. However, in these chemical systems phase diagrams show two crossing curves similar to Fig. 3; coexistence of the steady states occurs on one side of the crossing point and oscillations on the other side. We leave it open to relate (within a generalized theoretical framework) this low-dimensional phenomenon to our cross-shaped diagram in a high-dimensional system.

#### ACKNOWLEDGMENTS

This work was financially supported by the Deutsche Forschungsgemeinschaft (Grant No. Ma 629/6-1). M.S. and M.M. thank the Center for Mathematical Modeling (Santiago, Chile) for their hospitality and additional financial support.

- 
- [1] H.M. Jaeger, S.R. Nagel, and P. Behringer, *Rev. Mod. Phys.* **68**, 1259 (1996).
  - [2] *Disordered and Granular Media*, edited by D. Bideau and A. Hansen (North-Holland, Amsterdam, 1993).
  - [3] *Granular Matter*, edited by A. Mehta (Springer, Berlin, 1994).
  - [4] *Granular Gases*, edited by T. Pöschel and S. Luding (Springer, Berlin, 2001).
  - [5] A. Medina and C. Treviño, *J. Phys. Soc. Jpn.* **68**, 1883 (1999).
  - [6] W. Losert, D.G.W. Cooper, and J.P. Gollub, *Phys. Rev. E* **59**, 5855 (1999).
  - [7] S. Nasuno, A. Kudrolli, and J.P. Gollub, *Phys. Rev. Lett.* **79**, 949 (1997).
  - [8] R.A. Guyer, J. TenCate, and P. Johnson, *Phys. Rev. Lett.* **82**, 3280 (1999).
  - [9] A. Mehta, *Physica A* **186**, 121 (1992).
  - [10] J. Schäfer and D.E. Wolf, *Phys. Rev. E* **51**, 6154 (1995).
  - [11] A. Medina, E. Luna, R. Alvarado, and C. Treviño, *Phys. Rev. E* **51**, 4621 (1995).
  - [12] J. Rajchenbach, *Phys. Rev. Lett.* **65**, 2221 (1990).
  - [13] A. Mehta and G.C. Barker, *Europhys. Lett.* **56**, 626 (2001).
  - [14] M. Schmick, E. Goles, and M. Markus, *Phys. Rev. E* **62**, 397 (2000).
  - [15] M. Woltering and M. Markus, *Phys. Rev. Lett.* **84**, 630 (2000).
  - [16] J.C. Alexander, J.A. Yorke, Z. You, and I. Kan, *Int. J. Bifurcation Chaos Appl. Sci. Eng.* **2**, 795 (1992).
  - [17] Y.-C. Lai and C. Grebogi, *Phys. Rev. E* **52**, 3313 (1995).
  - [18] J.C. Sommerer and E. Ott, *Phys. Lett. A* **214**, 243 (1996).
  - [19] M. Woltering and M. Markus, *Phys. Lett. A* **260**, 453 (1999).
  - [20] J. M. Haile, *Molecular Dynamics Simulations* (Wiley, New York, 1992).
  - [21] M.A. Scherer, K. Kötter, M. Markus, E. Goles, and I. Rehberg, *Phys. Rev. E* **61**, 4069 (2000).
  - [22] K. Kötter, E. Goles, and M. Markus, *Phys. Rev. E* **60**, 7182 (1999).
  - [23] G. Kuwabara and K. Kono, *Jpn. J. Appl. Phys., Part 1* **26**, 1230 (1987).
  - [24] I. Goldhirsch and G. Zanetti, *Phys. Rev. Lett.* **70**, 1619 (1993).
  - [25] X. Nie, E. Ben-Naim, and S.Y. Chen, *Europhys. Lett.* **51**, 679 (2000).
  - [26] S.E. Esipov and T. Pöschel, *J. Stat. Phys.* **86**, 1385 (1997).
  - [27] J.S. Olafsen and J.S. Urbach, *Phys. Rev. Lett.* **81**, 4369 (1998).
  - [28] R.D. Wildman and D.J. Parker, *Phys. Rev. Lett.* **88**, 064301 (2002).
  - [29] M. Ding and W. Yang, *Phys. Rev. E* **54**, 2489 (1996).
  - [30] M. Sauer and F. Kaiser, *Int. J. Bifurcation Chaos Appl. Sci. Eng.* **6**, 1481 (1996).
  - [31] M. Franaszek, *Phys. Rev. A* **46**, 6340 (1992).
  - [32] E. Covas and R. Tavakol, *Phys. Rev. E* **55**, 6641 (1997).
  - [33] H. Sun, L. Ma, and L. Wang, *Phys. Rev. E* **51**, 3475 (1995).
  - [34] I.M. Kyprianidis, M.L. Petrani, J.A. Kalomiros, and A.N. Anagnostopoulos, *Phys. Rev. E* **52**, 2268 (1995).
  - [35] J. Boissonade and P. DeKepper, *J. Phys. Chem.* **84**, 501 (1980).
  - [36] I.R. Epstein and K. Showalter, *J. Phys. Chem.* **100**, 13 132 (1996).